ELSEVIER

Journal of Applied Geophysics 45 (2000) 63–81

JOURNAL OF APPLIED GEOPHYSICS

www.elsevier.nl/locate/jappgeo

Use of block inversion in the 2-D interpretation of apparent resistivity data and its comparison with smooth inversion

A.I. Olayinka [a,*,1], U. Yaramanci [b]

[a] *Department of Geology, University of Ibadan, Ibadan, Nigeria*

[b] *Department of Applied Geophysics, Technical University of Berlin, Ackerstr. 71-76, D-13355 Berlin, Germany*

Received 10 May 1999; accepted 19 May 2000

Abstract

The ability of a block inversion scheme, in which polygons are employed to define layers and/or bodies of equal resistivity, in determining the geometry and true resistivity of subsurface structures has been investigated and a simple strategy for deriving the starting model is proposed. A comparison has also been made between block inversion and smooth inversion, the latter being a cell-based scheme.

The study entailed the calculation (by forward modelling) of the synthetic data over 2-D geologic models and inversion of the data. The 2-D structures modelled include vertical fault, graben and horst. The Wenner array was used.

The results show that the images obtained from smooth inversion are very useful in determining the geometry; however, they can only provide guides to the true resistivity because of the smearing effects. It is shown that the starting model for block inversion can be based on a plane layer earth model. In the presence of sharp, rather than gradational, resistivity discontinuities, the model from block inversion more adequately represents the true subsurface geology, in terms of both the geometry and the formation resistivity. Field examples from a crystalline basement area of Nigeria are presented to demonstrate the versatility of the two resistivity inversion schemes.

Keywords: Resistivity inversion; Fault; Graben; Horst; Wenner array; Nigeria

1. Introduction

With the development of multi-electrode resistivity array, the collection of 2-D resistivity data is becoming increasingly popular for hydrogeological, environmental and geotechnical purposes (Griffiths and Barker, 1993). Although data collection is straight forward, the interpretation of the data can be difficult, due to the influence of equivalence, the robustness of the inversion algorithm and the number of layers or bodies used to model the data. Commercially available software applications are now routinely employed for inversion of 2-D apparent resistivity data. These programs can be classified into two groups, namely, smooth inversion and block inversion. Smooth inversion is a

* Corresponding author.

E-mail addresses: olayinka@skannet.com (A.I. Olayinka), yaramanci@tu-berlin.de (U. Yaramanci).

[1] Formerly at Department of Applied Geophysics, Technical University of Berlin, Ackerstr. 71-76, D-13355 Berlin, Germany.

0926-9851/00/$ - see front matter
PII: S0926-9851(00)00019-7

cell-based inversion while in block inversion polygons are employed to define layers and/or bodies of equal resistivity. The ability of these two inversion schemes in defining the geometry and true resistivity of subsurface structures, in the case where the resistivity increases with depth, is examined in this work. Typical 2-D geologic models investigated include vertical fault, graben and horst. These represent common targets in groundwater and environmental investigations in areas underlain by crystalline basement rocks.

A parallel can be drawn between smooth and block inversion schemes, for the 1-D and 2-D cases. In the classical approach to the 1-D interpretation of vertical electrical sounding data, it is tacitly assumed that the subsurface comprises a small (often less than 5) number of layers (Koefoed, 1979; Inman, 1985; Simms and Morgan, 1992; Muiuane and Pedersen, 1999). This, in essence, is a highly over-constrained problem and is analogous to a block inversion scheme in the 2-D case. On the other hand, in the approach popularized by Zohdy (1974, 1989), the model is overparameterized, with the number of layers in the interpreted model being equal to the number of electrode positions on the sounding curve. Such a strategy would produce a smooth model and has been extended to the interpretation of 2-D data (Barker, 1992; Loke and Barker, 1995).

An example of a smooth 2-D inversion algorithm is RES2DINV by Loke and Barker (1996), while the program RESIX IP2DI by Interpex (1996) is representative of a block inversion scheme. While the program RES2DINV is fully automatic, RESIX IP2DI requires that the interpreter prescribes an initial geological model as part of the input. This starting model is expected to be very close to the true model. In real cases, however, the true model is rarely, if ever, known precisely. It is demonstrated in this work that such a starting model could be based on a plane layer earth model. This simple approach has the added advantage that only the depth to the interface(s) need be varied as the inversion result is, for all practical purposes, not dependent on the resistivity contrast in the starting model. With the procedure, more than one model (for varying depths to the interface in the initial model) is produced which fit the same set of measured data. Some idea is thus provided of the range of 2-D equivalence.

The interpretation procedure described for block inversion is particularly suitable for the inversion of apparent resistivity pseudosection data from tropical and subtropical areas underlain directly by crystalline basement rocks. Apart from a thin soil cover which may not be well-resolved in 2-D surveys because of the relatively large electrode spacings used, a generalised vertical section in such areas comprises a low resistivity saprolite (derived from the in situ chemical weathering of the basement rocks) overlying a more resistant bedrock (Carruthers and Smith, 1992; Hazell et al., 1992). The block inversion process then invariably involves mapping the deviation of the true subsurface geology from the horizontal layering assumed in the starting model. Field examples from Nigeria are presented to demonstrate the usefulness of block inversion in interpreting real data.

2. Outline of method

2.1. Forward modelling of apparent resistivity pseudosection data

The apparent resistivity pseudosection data were generated by a 2-D forward modelling program, RESIX IP2DI, by Interpex (1996). The program uses a finite element approach to solve for the potential distribution due to point sources of current, and the potential distribution is converted into apparent resistivity values. The modelling routine accounts for 3-D sources (current electrodes) in a 2-D material model. This implies that the resistivity can vary arbitrarily along the line of surveying (x-direction) and with depth (z-direction), but the models

have an infinite perpendicular extension along the strike (y-direction). In all cases of the synthetic data, a layout with 81 electrodes was modelled with the Wenner array. The X- and Z-spacings are normalized with respect to the minimum electrode spacing A. In order to reduce the number of model parameters to be considered, the theoretical data have been limited to a single resistivity contrast of 1:20 between the overburden and the bedrock. Tests with several models indicate that the forward modelling program does not contain any systematic error. Moreover, the results are in agreement with those from another program RES2DMOD (Loke and Barker, 1996), which uses a finite difference method for the forward modelling.

Gauss distributed random noise with a standard deviation of 5% was added to the calculated responses for all the models in order to simulate field conditions. The synthetic apparent resistivity data were then inverted using a smooth and a block inversion scheme, respectively.

2.2. Smooth inversion

The program RES2DINV (Loke and Barker, 1996) was employed for the smooth inversion. A forward modelling subroutine is used to calculate the apparent resistivity values, and a non-linear least-squares optimisation technique is used for the inversion routine (DeGroot-Hedlin and Constable, 1990; Loke and Barker, 1996; Dahlin and Loke, 1998). The 2-D model used by the inversion program consists of a number of rectangular blocks whose arrangement is loosely tied to the distribution of the datum points in the pseudosection. The distribution and size of the blocks are automatically generated by the program so that the number of blocks do not exceed the number of datum points.

The inversion routine uses the Gauss–Newton method for a smoothness-constrained least-squares inversion, for which by default the vertical and horizontal smoothness constrains are the same (DeGroot-Hedlin and Constable, 1990). The smoothness constrain increases with 10% per layer, which along with increasing layer thickness reduces the resolution with depth. The inversion is based on an analytical calculation of the sensitivity matrix (Jacobian matrix) for a homogeneous halfspace and the sensitivity matrix is re-calculated using the finite element method at each step of the iteration. The optimisation equation (Ellis and Oldenburg, 1994b) can be represented as :

$$(\mathbf{J}_i^{\mathrm{T}}\mathbf{J}_i + \lambda_i \mathbf{C}^{\mathrm{T}}\mathbf{C})\boldsymbol{p}_i = \mathbf{J}_i^{\mathrm{T}}\boldsymbol{g}_i - \lambda_i \mathbf{C}^{\mathrm{T}}\mathbf{C}\boldsymbol{r}_{i-1} \qquad (1)$$

where $\mathbf{J}_i$ is the Jacobian matrix of partial derivatives, $\mathbf{J}_i^{\mathrm{T}}$ represents the transpose of $\mathbf{J}_i$, $\boldsymbol{g}_i$ is the discrepancy vector which contains the difference between the logarithms of calculated and observed apparent resistivity values, $\boldsymbol{p}_i$ is the perturbation vector to the model parameters, λ_i is a damping factor (or Lagrange multiplier) used to reduce the amplitude of $\boldsymbol{p}_i$, $\mathbf{C}$ is a flatness-filter matrix used to minimize the roughness of $\boldsymbol{p}_i$. The second term on the right-hand side of Eq. (1) applies the smoothness constraint directly on the model resistivity vector, $\boldsymbol{r}_{i-1}$. This guarantees that the model will be smooth subject to the damping factor used (Ellis and Oldenburg, 1994b). It also reduces the oscillations in the model resistivity values.

2.3. Block inversion

The interactive program RESIX IP2DI by Interpex (1996) was employed for the block inversion. This is a finite element forward and inverse modelling program that calculates the resistivity responses of 2-D earth models (Rijo, 1977; Petrick et al., 1977; Pelton et al., 1978). A finite element mesh is generated; each rectangular element is divided into four triangles and the resistivity of each triangle under the electrode spread is defined from the properties of the polygons which make up the model. The program uses ridge regression inversion (Inman,

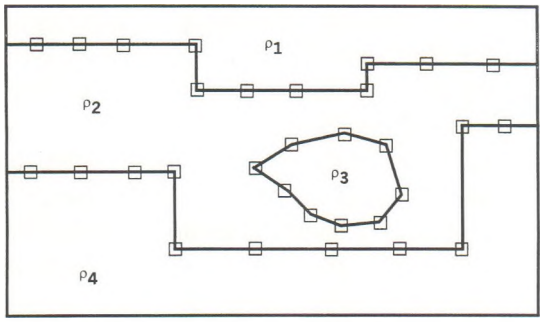

Fig. 1. Schematic representation of the input model in the block inversion algorithm, for an arbitrary shaped structure comprising a closed body and three layers.

1985) of polygon-based 2-D models to best fit the 2-D pseudosection data in a least squares sense.

With the aid of a mouse and using an interactive graphics screen, it is required that the interpreter creates a 2-D model defined by the vertices (i.e. the corners). The polygons (Fig. 1) can be constructed as a combination of up to 100 bodies and layers and up to 1000 vertices per model. Moreover, groups of vertices can be locked together to form a single unit whose x- and/or z-position can be used as an inversion parameter. The inversion is used to automatically improve the fit of the model by (automatically) adjusting some model parameters. As part of the inversion procedure, the body resistivity and position of vertices are allowed to change in the calculation and the user is able to specify which parameters to vary and which parameters to freeze. The finite element grid is determined from the number of electrodes and the electrode spacing. The program automatically creates a fine grid, which can be edited using the mouse. Vertical and horizontal elements can be inserted or deleted and elements can be split in half using the mouse.

The inverted parameters are given by :

$$\mathbf{P} = (\mathbf{G}^{\mathrm{T}}\mathbf{G} + k\mathbf{I})^{-1}\mathbf{G}^{\mathrm{T}}\boldsymbol{F}_{\mathrm{h}} \qquad (2)$$

for a weighted matrix $\mathbf{G}$ containing the derivatives of each data point with respect to each model parameter; T denotes transpose, $\mathbf{I}$ is the identity matrix; $\boldsymbol{F}_{\mathrm{h}}$ is the data vector. The matrix $\mathbf{G}$ is overdetermined as there are more data than parameters. The $\mathbf{G}^{\mathrm{T}}\mathbf{G}$ is square, symmetric and positive definite. k is a small positive constant which is added to the diagonal terms of the $\mathbf{G}^{\mathrm{T}}\mathbf{G}$ before inversion and has the effect of damping the small eigenvalues of $\mathbf{G}^{\mathrm{T}}\mathbf{G}$ which otherwise cause instability, while at the same time it has minor effect on the larger eigenvalues associated with the more well-determined parameters. Several values of k on a logarithmic scale are tried while iterating towards a solution, in order to minimize the least-squares residual. If the vector $\boldsymbol{e}$ is defined as $\boldsymbol{F}_{\mathrm{h}} - \boldsymbol{F}_{\mathrm{t}}$ (i.e. the difference between the measured data $\boldsymbol{F}_{\mathrm{h}}$ and the model data $\boldsymbol{F}_{\mathrm{t}}$), the residual sum of squares for the ridge regression solution is given by:

$$S = (\mathbf{e})^{\mathrm{T}}\mathbf{e} \qquad (3)$$

Marquardt's (1963) algorithm determines the smallest value of k for which the ridge regression estimator of Eq. (2) will yield a new model that better fits the field data. As the inversion process nears a solution or a minimum in the

Table 1
Definition of model parameters used in this work

A	minimum electrode spacing
Z	depth
$H_{(\mathrm{initial})}$	depth to the bedrock interface in the two-layer model used as starting model for block inversion
$\rho_{n(\mathrm{true})}$	the true resistivity of the nth layer
$\rho_{n(\mathrm{initial})}$	the prescribed resistivity of the nth layer for the initial model
$\rho_{n(\mathrm{model})}$	the resistivity of the nth layer after the data rms misfit has converged in block inversion

residual sum of squares (Eq. 3), successively smaller values of k are used.

Trial tests with several synthetic data have shown that the initial model for the block inversion can be based on a simple horizontal layer model. Several examples of these are presented in the following section. The effects of both the depth to the bedrock interface and the layer resistivities in the initial model on the inversion results are described. The model parameters used in this work are given in Table 1.

3. Theoretical examples

The model responses of some idealized 2-dimensional structures of geological relevance were calculated using the 2-D finite element forward modelling program. The calculated model responses, with 5% Gaussian noise added, were used as input for the 2-D inversion routines. In the discussion that follows, the inversion process was terminated when the difference in the data rms misfit between any two successive iterations was less than 3%. Calculation of the data misfit involves a comparison, for the respective datum points, between the observed apparent resistivities ($\rho_{a\,(obs)}$) and the calculated values($\rho_{a\,(calc)}$), as:

$$D_i = \left[\left(\rho_{a(obs)} - \rho_{a(calc)} \right) / \rho_{a(obs)} \right] \cdot 100\%$$

For the entire pseudosection the data rms misfit, D_{rms}, is given, as

$$D_{rms} = \left[1/N \Sigma D_i^2 \right]^{1/2}$$

3.1. Vertical fault

An example of the apparent resistivity pseudosection data calculated for a vertical fault model is presented in Fig. 2a. The depth to the top of the fault is 1 A and the fault throw is 4 A. Gaussian noise with an amplitude of 5% was added. There is a steepening of the isoresistivity contours at the position of the fault. The apparent resistivity data set was inverted, first with the smooth inversion program (RES2DINV) and next with the block inversion program (RESIX IP2DI).

During the smooth inversion of the data, the data rms misfit converged at the end of the fourth iteration. The geometry of the structure is better defined after inversion with respect to the very steep resistivity anomaly at about the position of the fault (Fig. 2b). There are portions of the overburden where the model resistivity is higher than the true value while over the remaining portion the model resistivities are lower than the true value. The same is true for the model bedrock resistivity. These are due to the smearing effects produced by smooth inversion, especially in the vicinity of zones with an abrupt discontinuity in resistivity.

A two-layer model was employed as the initial (starting) model for the block inversion. The effect of the depth to the bedrock interface in the initial model on the block inversion was investigated with a structure in which the model parameters include $\rho_{1(initial)} = 150\ \Omega m$ and $\rho_{2(initial)} = 1000\ \Omega m$. The $H_{(initial)}$ was varied from 1 A to 6 A. It was not possible to obtain a reasonable interpretation in the case with $H_{(initial)} = 1\ A$. The best-fit model in this case is shown in Fig. 2d. The pseudosection data calculated from this model (Fig. 3a) is to a very large extent "out-of-phase" with the synthetic observed data in Fig. 2a as reflected in the very high data rms misfit. The data misfit section (Fig. 3b) shows that there are two broad regions with negative data misfits, namely, at very shallow spacings in the upthrown block and at intermediate-to-large spacings in the downthrown side. On the other hand, there is a near-surface region with positive data misfits to the right-hand side of the fault. Hence, the data misfit is not evenly distributed over the entire section.

An acceptable interpretation, as indicated by a D_{rms} value of about the same level as the amount of Gaussian noise in the data, was produced from the block inversion for larger $H_{(initial)}$. The fault contact is correctly positioned

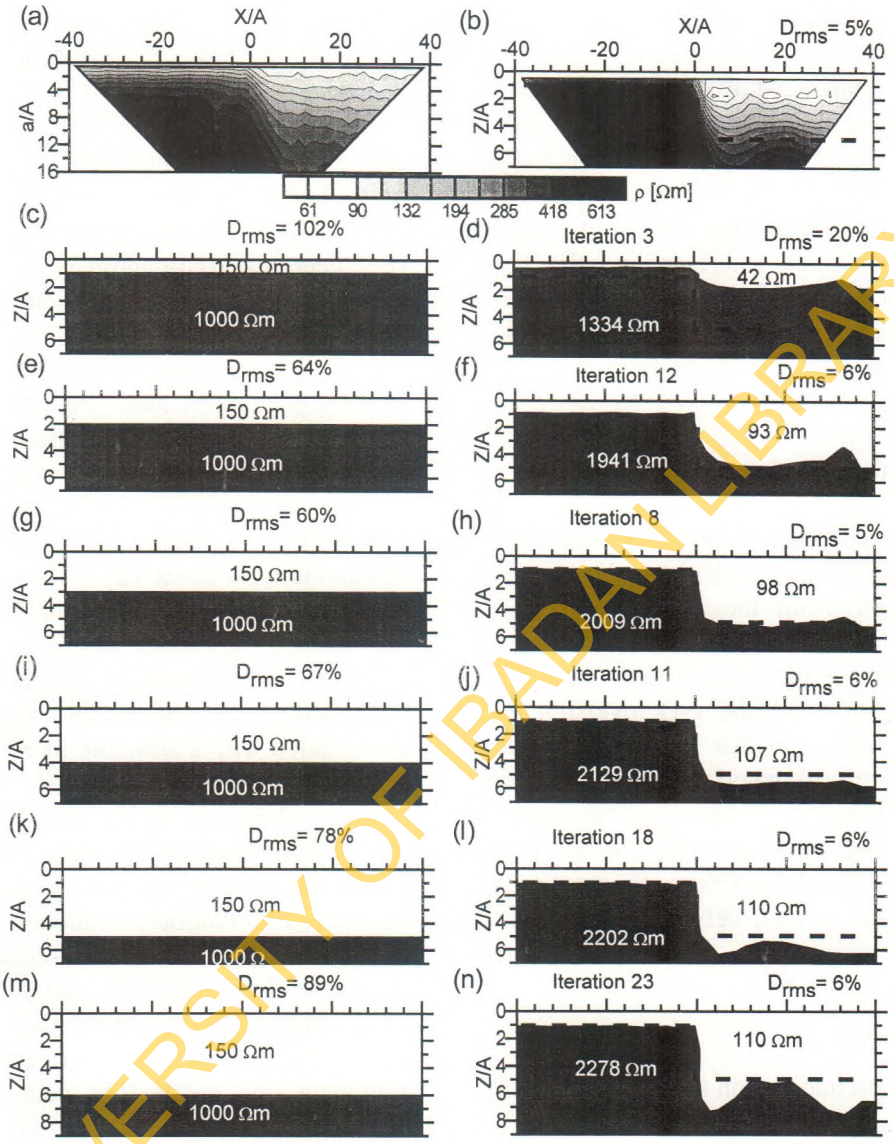

Fig. 2. (a) Synthetic pseudosection data calculated for a vertical fault structure, buried by a single overburden unit, with 5% Gaussian noise added. (b) Resistivity image obtained from smooth inversion algorithm. From (c) to (n), the left-hand panel is the starting model used as input for block inversion while the right-hand panel is the inverted model. The dashed line is an outline of the true 2-D model.

and it can be observed that there is an increase in both the overburden and the bedrock resistivity with an increase in the prescribed $H_{(initial)}$. However, if the starting depth is too deep, the inversion results can be unstable. In such instances, the depth of the interface of the lower resistive layer in the inverted model begins to undulate, as if a type of ringing occurs. Beard and Morgan (1991) and Oldenburg and Li (1999) have also reported such unusual inversion effects at the edges of 2-D structures. On the other hand, test with several theoretical examples indicate that the inversion result is stable when the resistivity contrast is varied in the initial guess than when the layer thickness is varied.

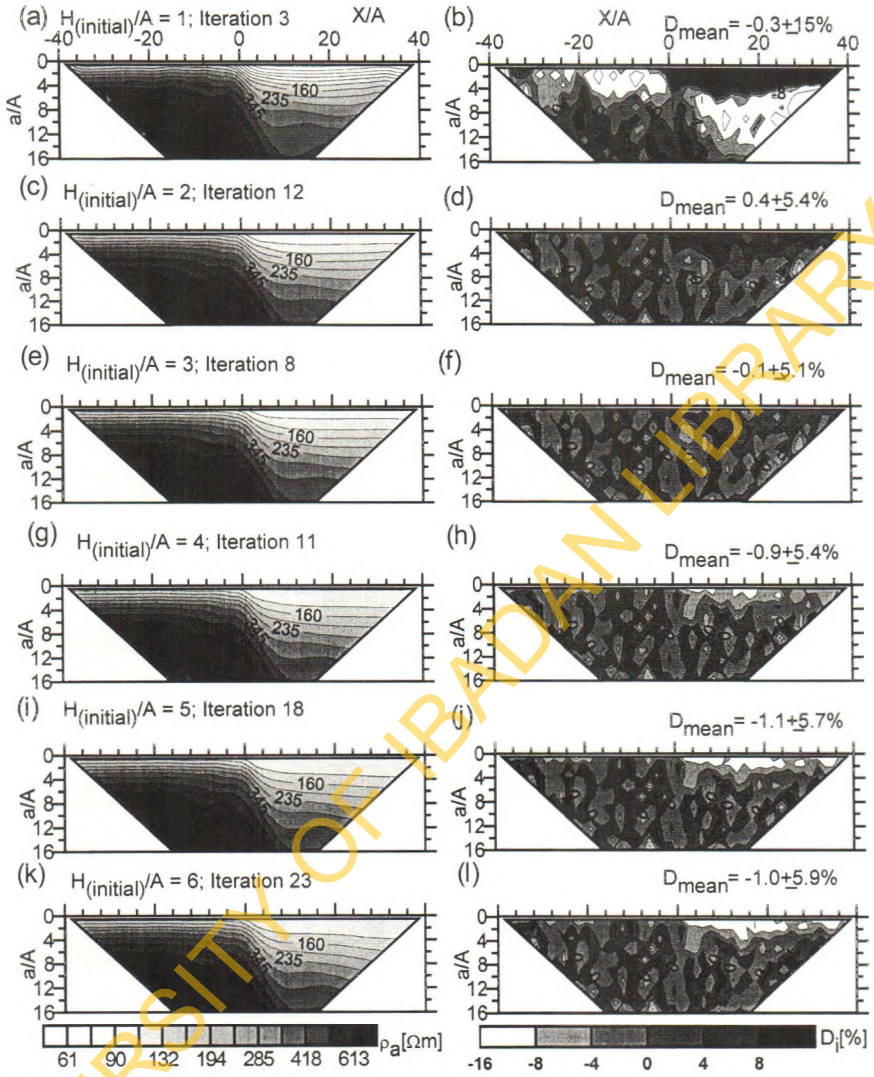

Fig. 3. The synthetic pseudosection data (left-hand panel) and the data misfit (right-hand panel) from some of the best-fit 2-D models from the block inversion of the data in Fig. 2.

3.2. Horst

The apparent resistivity pseudosection data calculated from a horst structure in which the depth to the top is $1A$ and the throw $4A$ is shown in Fig. 4a. The width of the body is $8A$. The overburden resistivity is 100 Ωm while that of the bedrock is 2000 Ωm. As would be expected, there is a highly resistive structure at the position of the horst. During the inversion of the apparent resistivity pseudosection data with the smooth inversion algorithm, the data rms misfit converged at the end of the fourth iteration and the high resistivity anomaly is correctly positioned (Fig. 4b).

The effect of the depth to bedrock interface in the initial two-layer model on the block inversion is shown in Fig. 4c–m, with $H_{(\text{initial})}$ varied from $1A$ to $6A$. In each case, the data rms misfit converged to about the same level as the amount of noise in the pseudosection data. There is a high resistivity anomaly at the posi-

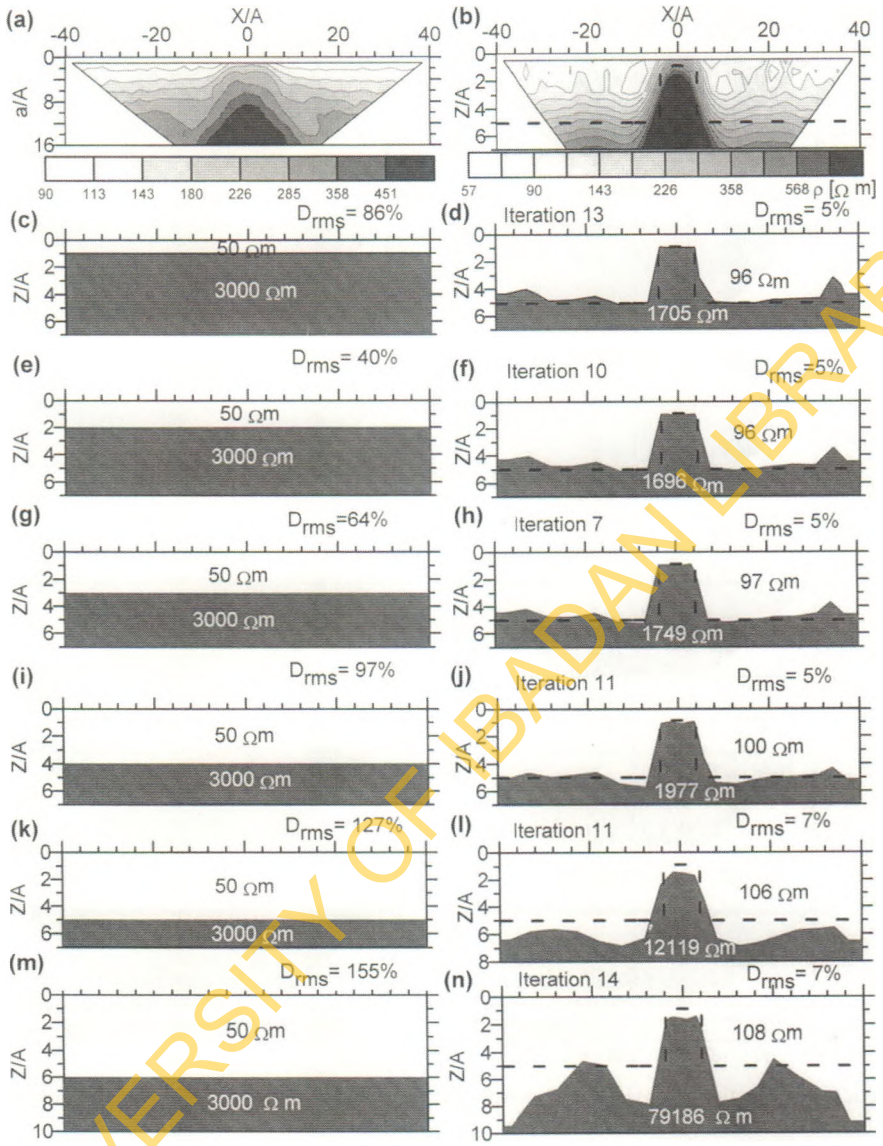

Fig. 4. Inversion of apparent resistivity data over a basement horst structure. The model parameters comprise depth to top $1A$, depth extent $4A$, width $8A$, overburden resistivity 100 Ωm and bedrock resistivity 2000 Ωm. (a) Synthetic data. (b) Model from smooth inversion. From (c) to (n), the left-hand panel is the starting model used as input for block inversion while the right-hand panel is the inverted model. The dashed line is an outline of the true 2-D model.

tion of the horst structure. The overburden resistivity is modelled accurately. The error in the estimate of the bedrock resistivity is very low up till an $H_{(\text{initial})}$ of $4A$. The inversion became unstable for larger $H_{(\text{initial})}$, and this is reflected in the very high bedrock model resistivity and the markedly undulatory bedrock interface. As with the fault model, variation in the resistivity contrast in the initial model has only a negligible effect on the inversion results.

3.3. Graben

The apparent resistivity pseudosection data calculated from a graben structure in which the depth to the top is $1A$ and the throw $4A$ is

shown in Fig. 5a. The width of the structure is 8 *A*. The overburden unit has a resistivity of 100 Ω and the bedrock 2000 Ωm. As would be expected, there is a low resistivity anomaly at the position of the graben. The model obtained from the smooth inversion of the pseudosection data is presented in Fig. 5b. The presence of a low resistivity anomaly at shallow depths and at the centre of the profile is clearly indicated, although it is difficult to fix the actual geometry of the bedrock contact.

To investigate the effect of the depth to bedrock interface in the two-layer model used as initial model for the block inversion of the apparent resistivity data, $H_{(initial)}$ was varied from 1 *A* to 6 *A*. The respective inverted models (Fig. 5c–n) show that in each case there is a low resistivity anomaly at the position of the

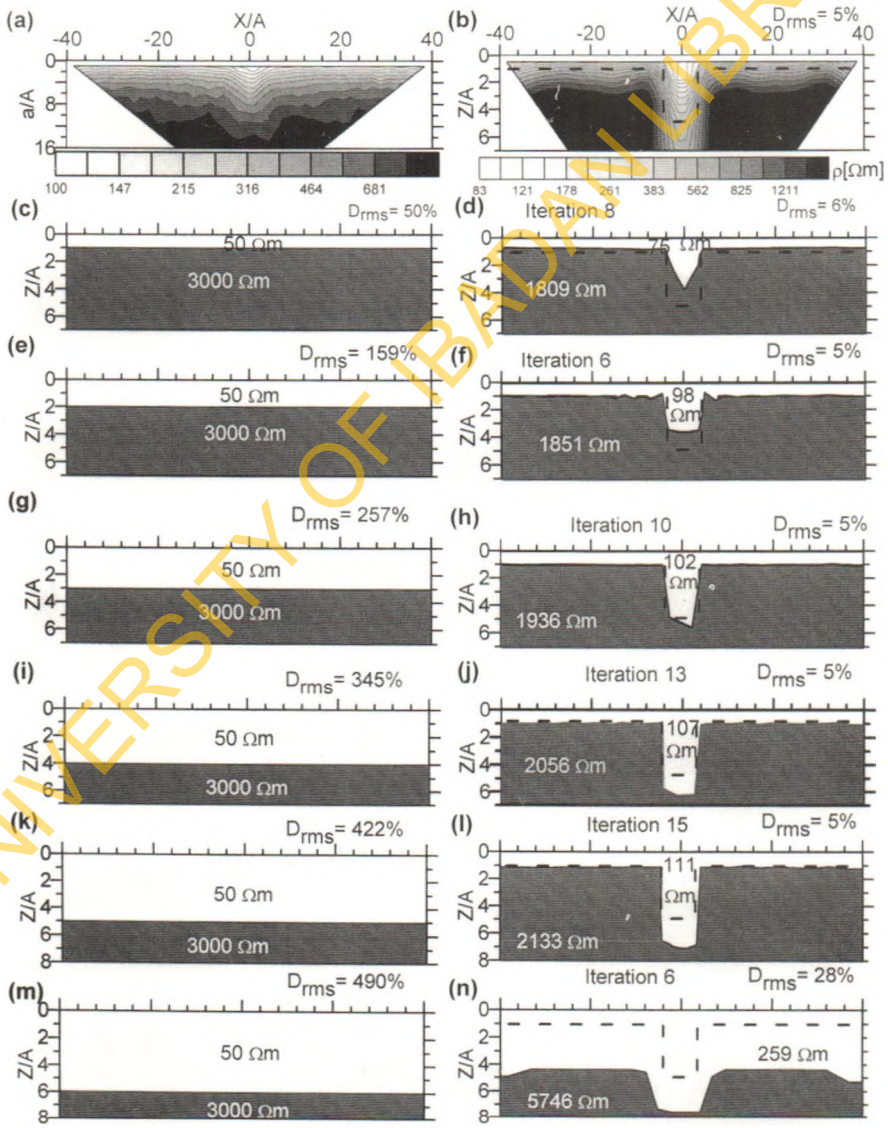

Fig. 5. Calculated pseudosection data for a trough structure with a width of 8 *A*, depth to top 1 *A*, depth to bottom 5 *A*, $\rho_1 = 100$ Ωm, $\rho_2 = 2000$ Ωm. (b) Model from smooth inversion. From (c) to (n), the left-hand panel is the initial model for block inversion while the right-hand panel is the respective inverted model.

graben structure. There is an increase in both the overburden and the bedrock resistivities as $H_{(initial)}$ increases. That the inverted model in Fig. 5n is in error is indicated by the very high data rms misfit. Test with several theoretical examples show that the inversion results are, for all practical purposes, not affected by the layer resistivities in the starting models.

4. Extension to three geoelectric units

The interpretation procedure described above was extended to 2-D models with two overburden units in order to study the influence of equivalence on the result obtained from data inversion. The pseudosection data in Fig. 6a was calculated from a structure in which there is

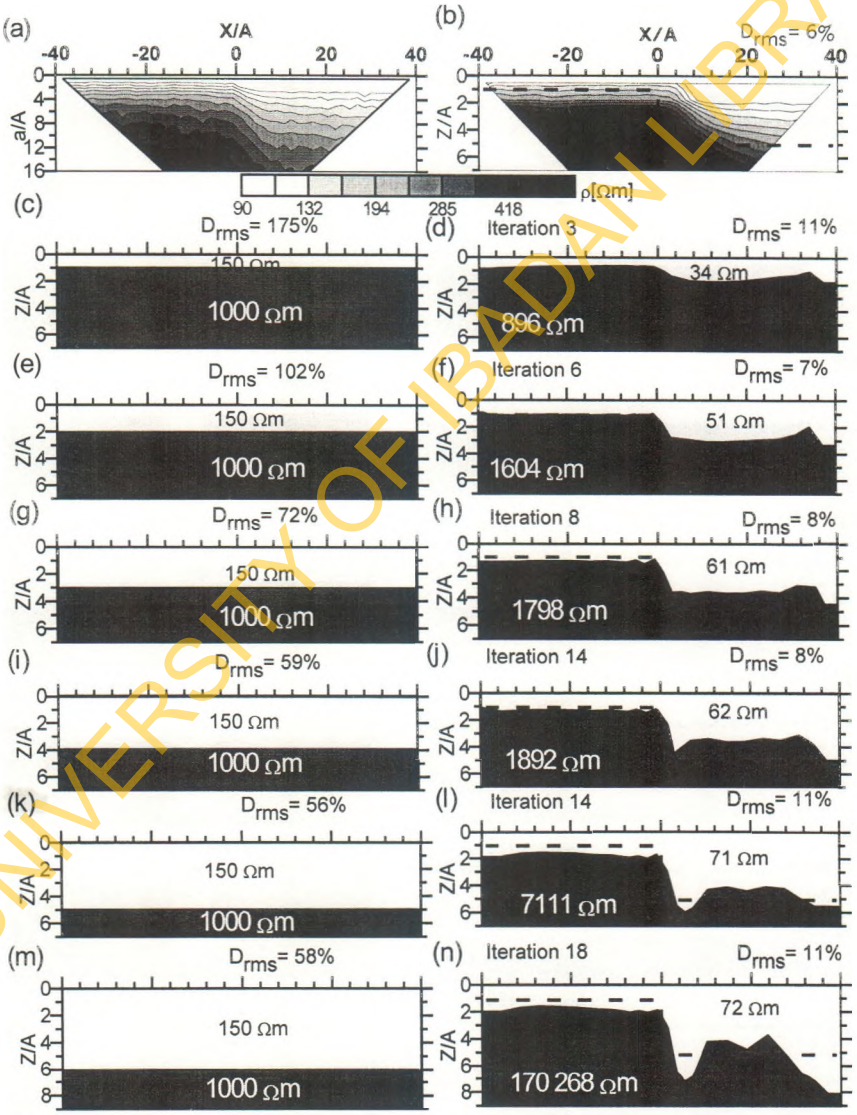

Fig. 6. The effect of the suppression of a thin surfacial layer on the modelling and inversion of the apparent resistivity data. (a) Synthetic data calculated over a fault model buried under two thin overburden units. (b) 2-D model obtained from the smooth inversion. From (c) to (n), the left-hand panel is the initial model for block inversion while the right-hand panel is the respective inverted model from block inversion.

a thin (0.5 A) surfacial relatively conductive layer with a resistivity of 30 Ωm. The underlying geoelectric unit has a resistivity of 100 Ωm. The depth to the top of the fault is 1 A while the throw is 4A. The bedrock resistivity is 2000 Ωm. There is a steepening of the contours in the vicinity of the buried fault. The model from the smooth inversion of the data (Fig. 6b) shows that the presence of the two overburden units has reduced the magnitude of the anomaly due to the buried fault.

A two-layer model was employed as the starting model for the block inversion. The depth to the bedrock interface was varied from 1 A to 6 A. As might be expected, the equivalent (or replacement) overburden resistivity in the inverted model is intermediate between the resistivities of the two overburden units in the true

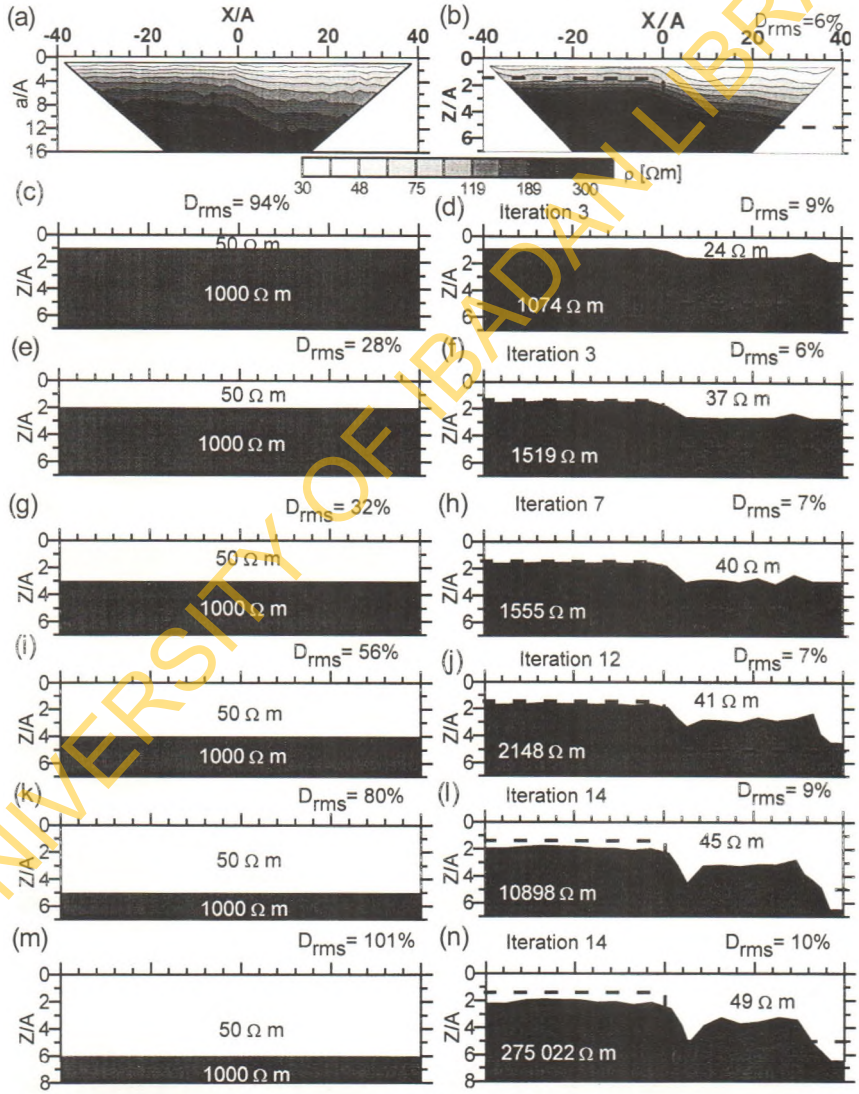

Fig. 7. Inversion of data in the presence of a relatively thick surficial layer. (a) Synthetic data calculated from the 2-D model. (b) 2-D model obtained from the smooth inversion. From (c) to (n), the left-hand panel is the initial model for block inversion while the right-hand panel is the respective model from the block inversion. An outline of the bedrock interface in the true model is shown in the inverted models.

model (Fig. 6c to n). The data rms misfit is relatively high for $H_{(initial)}$ of $1A$, indicating that the best-fit model in this case is "out-of-phase" with the measured data. For larger $H_{(initial)}$, up till $4A$, there is a decrease in the error of estimation of the bedrock model resistivity with an increase in $H_{(initial)}$. Although the fault contact is correctly located, there is a depth underestimation in the downthrown block. For larger $H_{(initial)}$, the inversion was unstable, with the data rms misfit and the bedrock model resistivity being relatively high.

If the thickness of the surfacial layer becomes substantial, it is to be expected that its influence on the pseudosection data, and consequently also, its effect on the inversion results, would become more pronounced. This is illustrated with a model in which the thickness of the surficial layer is $1A$ while its resistivity is 30 Ωm. The depth to the top of the fault is $1.5A$ while the throw is $3.5A$. The resistivity of the lower unit of the overburden is 100 Ωm while that of the basement is 2000 Ωm. Both the pseudosection data and the smooth inversion model (Fig. 7a and b, respectively) indicate that the anomaly is greatly suppressed. There is only a slight steepening isoresistivity contours at depth in the vicinity of the position of the fault.

A two-layer model was first employed as the starting model for the block inversion of the

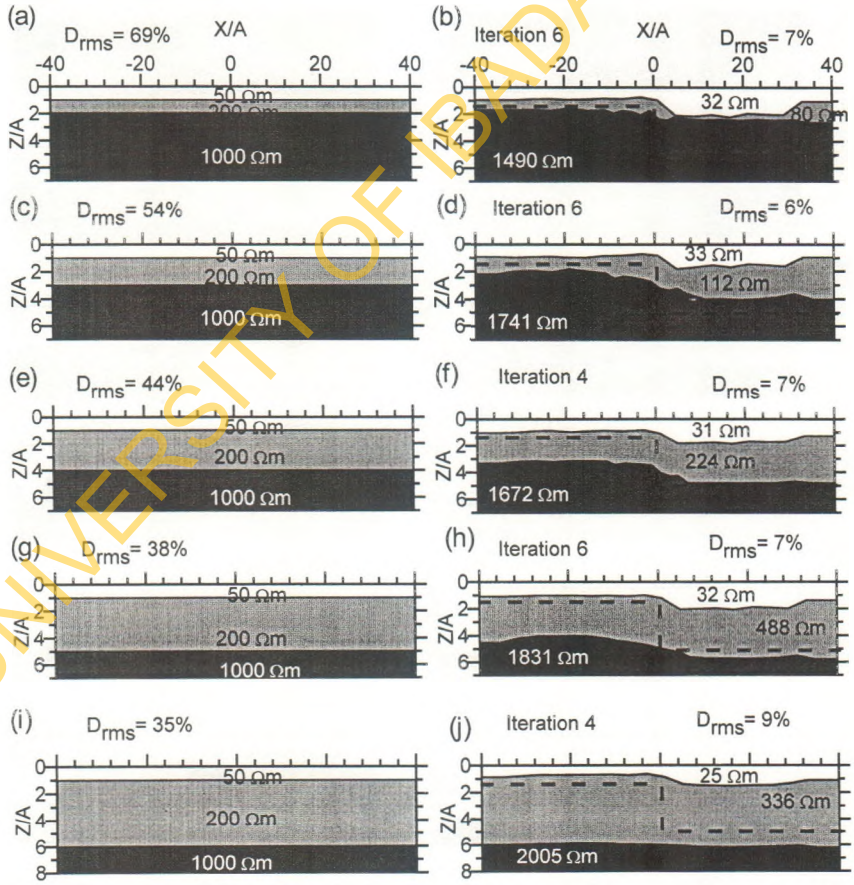

Fig. 8. Re-interpretation of the apparent resistivity data in Fig. 7a employing three geoelectric units. The left-hand panels are the initial models for block inversion while the corresponding inverted models are shown in the right-hand panels. Note that the data misfit is relatively high for the inverted model in (j).

data, with the $H_{(initial)}$ varied from 1 A to 6 A. The D_{rms} for the best-fit inverted model in Fig. 7d is relatively high and on account of this, the model is not considered acceptable. Similarly, the bedrock model resistivity for the inverted models in Fig. 7l and n are too high and, for this reason, these models are not considered equivalent interpretation of the synthetic observed data. On the other hand, the inversion results for moderate $H_{(initial)}$ (Fig. 7f, h and j) are reasonable interpretations of the data. It may be noted that even for these models, there is an underestimation of the depth to the bedrock interface in the downthrown block.

The apparent resistivity data in Fig. 7a were re-interpreted using an initial model comprising three layers in which the resistivities are 50, 200 and 1000 Ωm, respectively. The depth to the first interface is 1 A while that to the second interface was varied from 2 A to 6 A. The results obtained after the block inversion are presented in Fig. 8. It can be observed that the resistivity of the first geoelectrical unit is reliably estimated. However, the horizontal interface has been converted into a dipping structure as a result of the influence of the underlying faulted block. The model resistivity of the second geoelectric unit varies over a wide range. Similarly, the bedrock model resistivity varies over a wide range.

5. Field examples

The interpretation procedure described above has been tested with several case histories from the crystalline basement area of southwestern Nigeria (Fig. 9). The layer resistivities in the initial model for the block inversion have been prescribed based on the range of the measured pseudosection data. The resistivity of the upper layer is of the order of the minimum apparent resistivity (measured at the shallowest electrode spacing) and the bedrock resistivity prescribed as the maximum apparent resistivity (measured

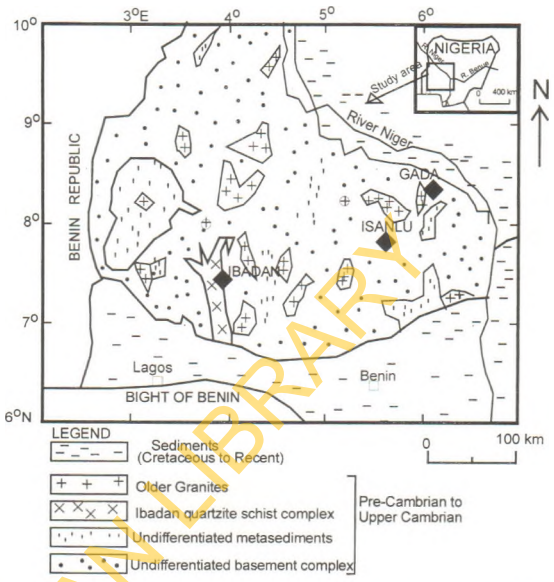

Fig. 9. Generalised geological map of southwestern Nigeria showing the study area. A map of Nigeria is presented as inset.

at the largest electrode spacing). Representative data sets from one of the sites are presented below.

The field data from Ibadan demonstrate the usefulness of both smooth and block inversion schemes in interpreting data from a low latitude area underlain by crystalline basement rocks. The major rock types in the study area include Older granites, quartzite and quartz-schist, gneisses and undifferentiated metasediments of Pre-Cambrian to Upper Cambrian age. These are often overlain by a thin veneer of regolith materials derived from the chemical weathering of the basement rocks.

Wenner apparent resistivity pseudosection data were measured as part of a programme involving five electrical imaging lines and hydrochemical analyses, to determine the gross layered structure and environmental impact of an urban waste dump. The solid geology comprises quartzite and quartz-schist. The minimum spacing was 10 m and the maximum 60 m. Two of the lines are discussed in this paper to highlight the range of 2-D equivalent models that

are possible from the same set of measured data.

Line 3 is one of the lines measured on the waste dump; the data are between 4 and 90 Ωm and there is a low resistivity anomaly between about 120 and 180 m (Fig. 10a). The model obtained from the smooth inversion of the field data (Fig. 10b) indicates a low resistivity material (i.e. the refuse plus leachate) overlying a highly resistant bedrock. However, it is difficult to place the refuse-bedrock contact. Consequently, as a final step in the interpretation, block inversion of the data was carried out.

An examination of the vertical sets of apparent resistivities (for successive electrode spacings) beneath each electrode position shows that

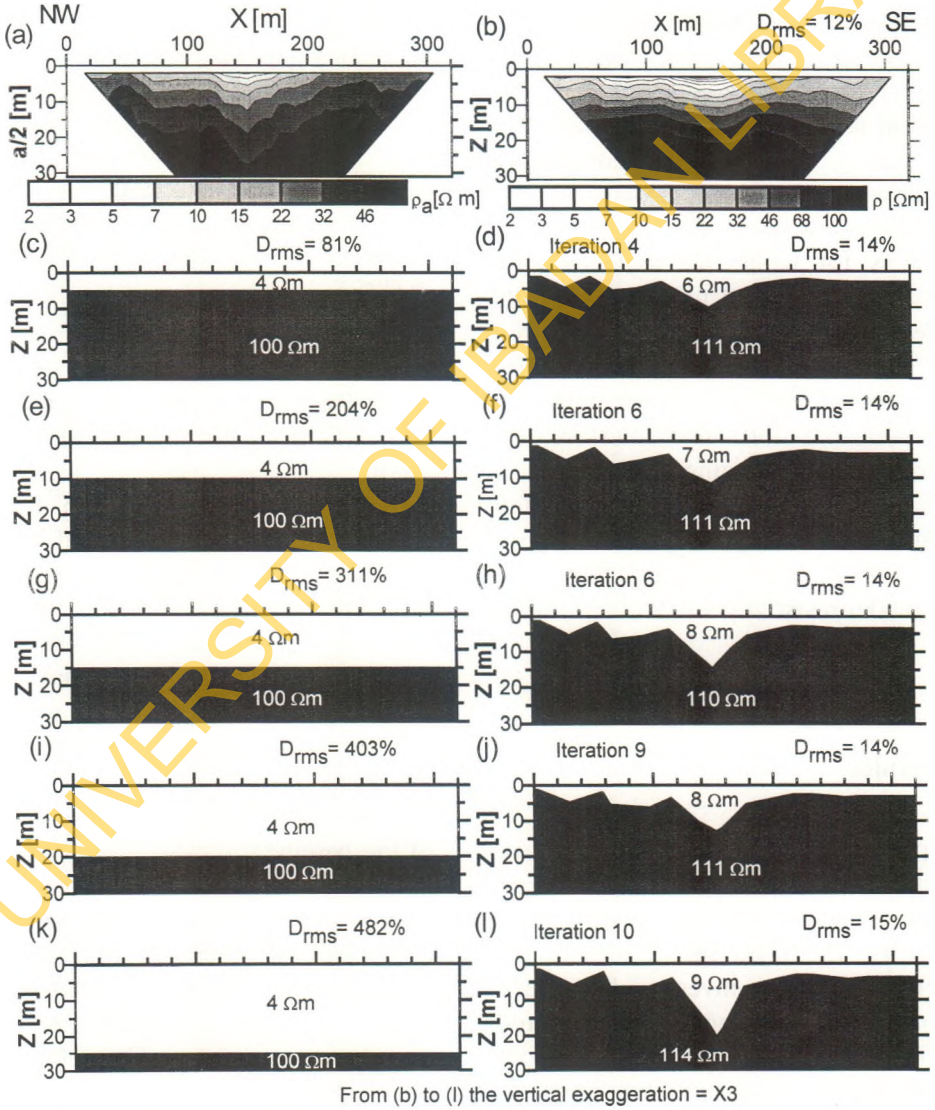

Fig. 10. Interpretation of Wenner pseudosection data (line 3) from a waste dump site, Ibadan, southwestern Nigeria. (a) Measured data. (b) Model from smooth inversion. From (c) to (l), the left-hand panel is the initial model for block inversion while the right-hand panel is the respective inverted model.

there is a very steep vertical gradient, supporting a strong possibility of a sharp, rather than a gradational, vertical resistivity change. A two-layer initial model was prescribed in which the

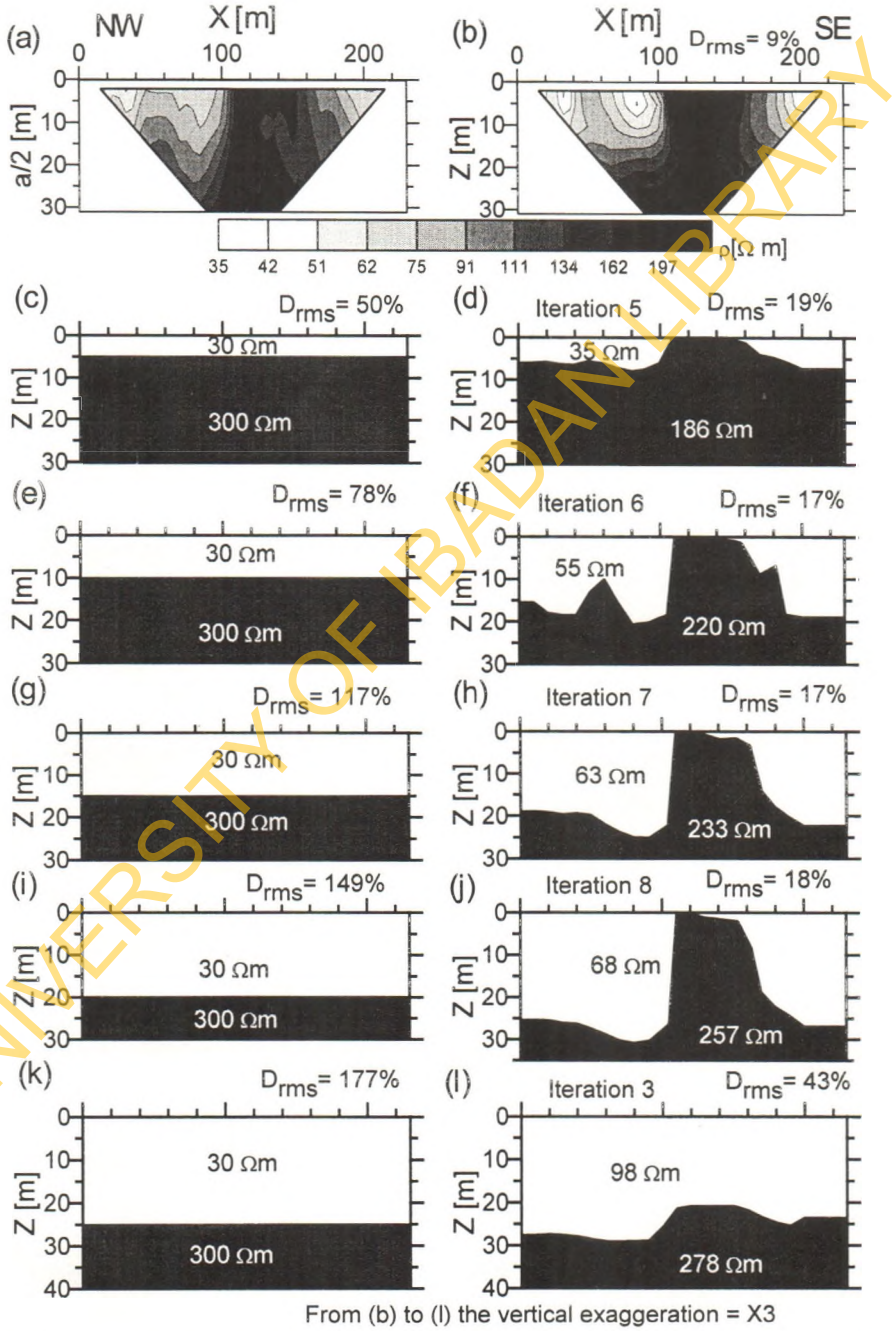

Fig. 11. Interpretation of Wenner pseudosection data (line 5) adjacent to the Ibadan waste dump site. (a) Measured data. (b) Model from smooth inversion. From (c) to (l), the left-hand panel is the initial model for block inversion while the right-hand panel is the respective inverted model.

resistivity of the upper layer is 4 Ωm while that of the bedrock is 100 Ωm.

The data rms misfit converged to between 14% and 15% in all the models tested, which is in very good agreement with the result from the smooth inversion. The resistivity of the upper layer (representing the refuse) shows a slight increase as the thickness of the upper layer in the initial model was increased. This was accompanied by an increase in the maximum thickness of the layer from about 10 m in Fig. 10d to about 18 m in Fig. 10l. The ratio of the thickness to the resistivity of the layer (i.e. its conductance) probably remained constant from one inverted model to the other. The bedrock model resistivity varies within a narrow range at between 110 and 114 Ωm. These indicate that the resistivities of both geoelectrical units are

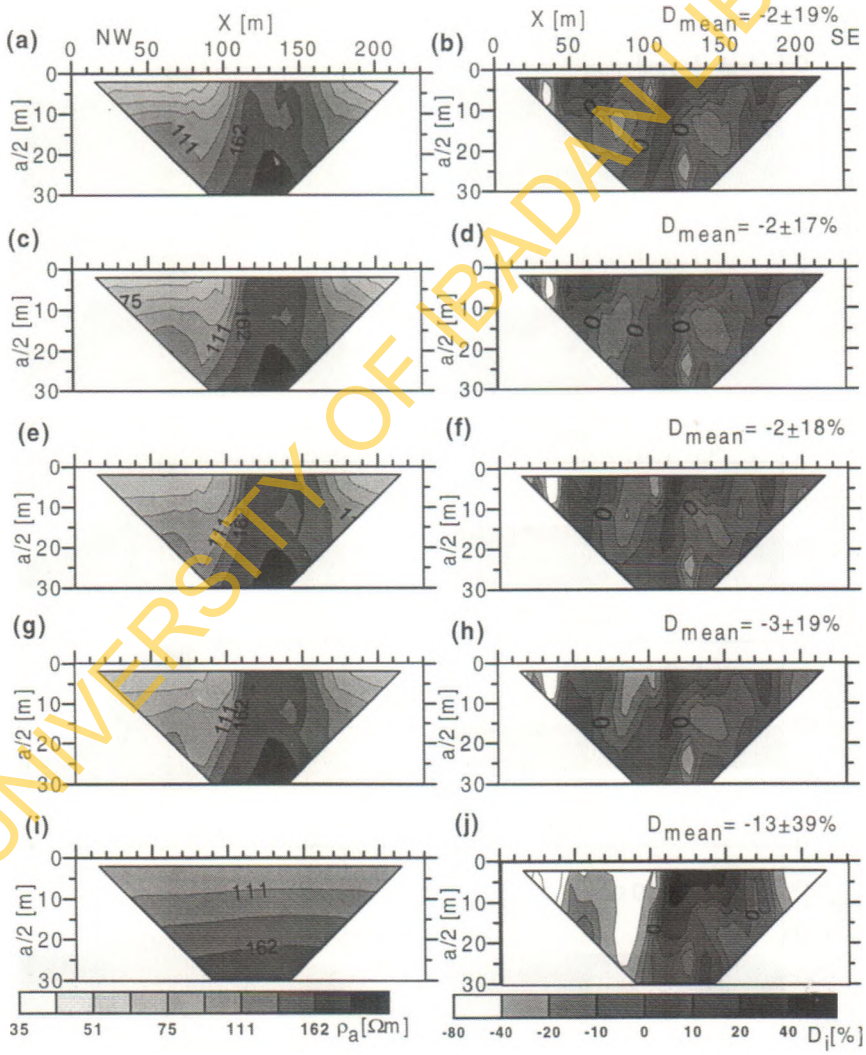

Fig. 12. The synthetic pseudosection data (left-hand panel) and the data misfit (right-hand panel) from the best-fit 2D models from the block inversion of the data in Fig. 11. (a,b) $H_{(initial)} = 5$ m. (c,d) $H_{(initial)} = 10$ m. (e,f) $H_{(initial)} = 15$ m. (g,h) $H_{(initial)} = 20$ m. (i,j) $H_{(initial)} = 25$ m.

well constrained. Similar results were obtained with other initial models tested using different starting resistivities for both the overburden and the bedrock.

The field data presented in Fig. 11a were measured near, but outside, the waste dump site. Here, the apparent resistivities are higher at between 35 and 253 Ωm. A high resistivity structure is prominent between 110 and 160 m, this coinciding with the outcrop of the weathered basement materials. The model obtained from the smooth inversion of the data is presented in Fig. 11b, with the usual smearing effect noticeable.

In the block inversion, a two-layer model with resistivities of 30 and 300 Ωm, respectively, was used in modelling the data. The depth to interface was varied between 5 and 25 m. The data rms misfit is within the range of 17% and 19% for $H_{(\text{initial})}$ up till 20 m. The overburden model resistivity varies by a factor of about 2 while the bedrock model resistivity varies by a factor of about 1.4. The thickness of the weathering profile in the zone flanking the horst-like structure is expected to range between about 7 and 30 m. The data rms misfit for an $H_{(\text{initial})}$ of 25 m converged to a very high value, indicating that the inverted model (Fig. 11l) is not an acceptable interpretation of the field data.

The synthetic pseudosection data calculated from the best-fit smooth inversion models in Fig. 11, as well as the corresponding data misfits, are presented in Fig. 12. It can be observed that the data misfits are low and randomly distributed. However, for Fig. 12j there is an overestimation of the apparent resistivities (negative D_i) on the western flank of the high resistivity body. This is due to the very high overburden model resistivity for this model. Moreover, there is an underestimation of the apparent resistivities at the position of the horst structure as expected from the excessive depth to the top of the horst structure.

It should be noted that in this example, the resistivities of the geoelectrical units are reasonably well constrained. Test with other starting models show that the resistivity contrast in the initial model has only a negligible effect on the inversion results.

6. Discussion and conclusions

In this paper, a comparison has been made between inversion results with smooth and block inversion schemes. It should be stressed that all inversion methods make assumption(s) about the resistivity distribution of the subsurface which are implemented in the form of constrains. The accuracy of the results depends to a large extent on whether or not the actual subsurface agrees with these assumptions. The smoothness-constrained method assumes the subsurface resistivity varies in a smooth manner and it attempts to minimise the changes in resistivity in a least-squares sense. In cases where the subsurface resistivity varies in a smooth manner, for example chemical pollution plumes (Barker, 1996), this approach will perform very well. On the other hand, the block inversion method assumes that the subsurface consists of a few homogeneous regions with a sharp interface between them. Such an inversion scheme would be the logical choice where the subsurface comprises units with sharp boundaries in order to determine both layer boundary locations and layer resistivities accurately (Ellis and Oldenburg, 1994a; Smith et al., 1999). The synthetic examples chosen for this paper agree exactly with the assumptions made by the block inversion method (and hence performed well).

Test with field data from the crystalline basement area of southwestern Nigeria has shown that the block inversion method gives very good results if the actual subsurface consists of two homogeneous regions with a sharp interface and if the starting depth of the two-layer model is reasonably accurate. If the subsurface is more complicated with several regions, or if the starting depth is too shallow or too deep, the results can be unstable. It has been shown that in such cases the depth of the interface of the lower

resistive layer in the inverted model begins to undulate, as if a type of ringing occurs. Beard and Morgan (1991) and Oldenburg and Li (1999) have also described such unusual inversion effects at the edges of 2-D structures. These weaknesses can be easily overcome by a combined use of a cell-based inversion method and the block inversion method. The cell-based inversion will at least give a rough idea of the bedrock depth which will prevent the starting depth in the block inversion to be too shallow or too deep, particularly with field data. The cell-based inversion model can also warn the user if the subsurface is more complex than the two regions model. The different inversion methods described can be viewed as complementary tools the interpreter can employ to obtain the most consistent and reasonable results for a given data set.

Acknowledgements

This work was carried out in the Department of Applied Geophysics, Technical University, Berlin. The authors are grateful to the Alexander von Humboldt Foundation, Bonn, who funded AIO as research fellow. Les P. Beard, Editor-in-Chief N.B. Christensen and an anonymous reviewer are thanked for their suggestions which greatly improved the paper.

References

Barker, R.D., 1992. A simple algorithm for electrical imaging of the subsurface. First Break 10 (2), 53–62.

Barker, R.D., 1996. Application of electrical tomography in groundwater contamination studies. EAGE 58th Conference and Technical Exhibition Extended Abstracts. p. P082.

Beard, L.P., Morgan, F.D., 1991. Assessment of 2-D resistivity structures using 1-D inversion. Geophysics 56, 874–883.

Carruthers, R.M., Smith, I.F., 1992. The use of ground electrical survey methods for siting water-supply boreholes in shallow crystalline basement terrains. In: Wright, E.P., Burgess, W.G. (Eds.), Hydrogeology of Crystalline Basement Aquifers in Africa. Geological Society Special Publication No. 66, pp. 203–220.

Dahlin, T., Loke, M.H., 1998. Resolution of 2D Wenner resistivity imaging as assessed by numerical modelling. J. Appl. Geophys. 38, 237–249.

DeGroot-Hedlin, C., Constable, C., 1990. Occam's inversion to generate smooth two-dimensional models from magnetotelluric data. Geophysics 55, 1613–1624.

Ellis, R.G., Oldenburg, D.W., 1994a. Applied geophysical inversion. Geophys. J. Int. 116, 5–11.

Ellis, R.G., Oldenburg, D.W., 1994b. The pole–pole 3D DC resistivity inverse problem: a conjugate-gradient approach. Geophys. J. Int. 119, 187–194.

Griffiths, D.H., Barker, R.D., 1993. Two-dimensional resistivity imaging and modelling in areas of complex geology. J. Appl. Geophys. 29, 211–226.

Hazell, J.R.T., Cratchley, C.R., Jones, C.R.C., 1992. The hydrogeology of crystalline aquifers in northern Nigeria and geophysical techniques used in their exploration. In: Wright, E.P., Burgess, W.G. (Eds.), Hydrogeology of Crystalline Basement Aquifers in Africa. Geological Society Special Publication No. 66, pp. 155–182.

Inman, J.R., 1985. Resistivity inversion with ridge regression. Geophysics 50, 2112–2131.

Interpex, 1996. RESIX IP2DI v3, Resistivity and induced polarization data interpretation software. Interpex, Golden, Colorado.

Koefoed, O., 1979. Geosounding Principles: 1. Resistivity Sounding Measurements. Elsevier, Amsterdam, 276 pp.

Loke, M.H., Barker, R.D., 1995. Improvements to the Zohdy method for the inversion of resistivity sounding and pseudosection data. Comput. Geosci. 21 (2), 321–332.

Loke, M.H., Barker, R.D., 1996. Rapid least-squares inversion of apparent resistivity pseudosections by a quasi-Newton method. Geophys. Prospect. 44, 131–152.

Marquardt, D.W., 1963. An algorithm for least-squares estimation of nonlinear parameters. J. Soc. Ind. Appl. Math. 11, 431–441.

Muiuane, E.A., Pedersen, L.B., 1999. Automatic 1D interpretation of DC resistivity sounding data. J. Appl. Geophys. 42, 35–45.

Oldenburg, D.W., Li, Y., 1999. Estimating depth of investigation in dc resistivity and IP surveys. Geophysics 64, 403–416.

Pelton, W.H., Rijo, L., Swift, C.M., 1978. Inversion of two-dimensional resistivity and induced-polarization data. Geophysics 43, 788–803.

Petrick, W.R., Pelton, W.H., Ward, S.H., 1977. Ridge regression applied to crustal resistivity sounding data from South Africa. Geophysics 42, 995–1005.

Rijo, L., 1977. Electromagnetic modeling by the finite element method. PhD thesis, University of Utah.

Simms, J.E., Morgan, F.D., 1992. Comparison of four

least-squares inversion schemes for studying equivalence in one-dimensional resistivity interpretation. Geophysics 57, 1282–1293.

Smith, T., Hoversten, M., Gasperikova, E., Morrison, F., 1999. Sharp boundary inversion of 2D magnetotelluric data. Geophys. Prospect. 47, 469–486.

Zohdy, A.A.R., 1974. Use of Dar Zarrouk curves in the interpretation of vertical electrical sounding data. US Geol. Surv. Bull. 1313-D, 41.

Zohdy, A.A.R., 1989. A new method for the automatic interpretation of Schlumberger and Wenner sounding curves. Geophysics 54, 245–253.